Proc. Natl. Acad. Sci. USA
Vol. 88, pp. 4518–4522, May 1991
Biochemistry

Active conformation of an insect neuropeptide family

(pyrokinin/β-turn/molecular dynamics/NMR/pheromone)

RONALD J. NACHMAN*†, VICTORIA A. ROBERTS†, H. JANE DYSON†, G. MARK HOLMAN*, AND JOHN A. TAINER†‡

*Veterinary Toxicology and Entomology Research Laboratory, Agricultural Research Service, U.S. Department of Agriculture, Route 5, Box 810, College Station, TX 77840; and †Department of Molecular Biology, Research Institute of Scripps Clinic, La Jolla, CA 92037

Communicated by Floyd E. Bloom, January 31, 1991

ABSTRACT **To understand the structural and chemical basis for insect neuropeptide activity, we have designed, synthesized, and determined the conformation of a biologically active cyclic analog of the pyrokinins, an insect neuropeptide family that mediates myotropic (visceral muscle contractile) activity. Members of this insect neuropeptide family share the common C-terminal pentapeptide sequence Phe-Xaa-Pro-Arg-Leu-NH_2 (Xaa = Ser, Thr, or Val). Circular dichroic, nuclear magnetic resonance, and molecular dynamics analyses of the conformationally restricted cyclic pyrokinin analog cyclo(-Asn-Thr-Ser-Phe-Thr-Pro-Arg-Leu-) indicated the presence of a β-turn in the active core region encompassing residues Thr-Pro-Arg-Leu. The rigid cyclic analog retains biological activity, suggesting that its C-terminal β-turn is the active pyrokinin conformation recognized by the myotropic receptor. As individual pyrokinins and pyrokinin-like neuropeptides demonstrate both oviduct-contractile and pheromone-biosynthesis activities in various insects, the biologically active β-turn structure reported here holds broad significance for many biological processes.**

Insect neuropeptides mediate many critical processes such as pheromone production, diuresis, visceral muscle contraction (myotropic activity), blood sugar level, mating, and pupal development (1). Yet, a complete characterization of these biologically active peptides has proved extremely difficult. Nearly six decades passed between the first investigations into the role of neuropeptide hormones in insect physiology by Kopec in 1917 (2) and the first report of the isolation and sequence analysis of an insect neuropeptide in 1975 (3). Moreover, despite the large number of insect neuropeptides that have been identified since then, no active conformation of an insect neuropeptide or analog has yet been determined.

The pyrokinin insect neuropeptides are particularly suitable for complete characterization because they stimulate contractions of cockroach proctodeum (hindgut) and oviduct, and their myotropic activity can be readily tested with the isolated hindgut bioassay (4), which is both rapid and reproducible. Leucopyrokinin (LPK), pGlu-Thr-Ser-Phe-Thr-Pro-Arg-Leu-NH_2, is isolated from heads of the Madeira cockroach (*Leucophaea maderae*) (4), where it is found in the corpora cardiaca, a neurosecretory organ analogous to the pituitary and hypothalamus glands of the vertebrate endocrine system. Three related neuropeptides from the locust are more potent stimulators of oviduct than hindgut contraction (5, 6). In this paper, we report the active conformation of a cyclic pyrokinin analog determined by both experimental and computational techniques. The tight constraints on the active core structure of this cyclized peptide, which maintains biological activity despite its relative rigidity, suggest that this is the conformation recognized by the myotropic receptor. The rational approach to peptide design used here has proved useful for other peptide ligands (7).

The publication costs of this article were defrayed in part by page charge payment. This article must therefore be hereby marked "*advertisement*" in accordance with 18 U.S.C. §1734 solely to indicate this fact.

MATERIALS AND METHODS

Peptide Synthesis. The C-terminal acid LPK analog ([Asn^1]LPK-OH) was synthesized and purified (8) with a retention time of 25.9 min on a μ-Bondapak phenyl HPLC column and found to have the amino acid analysis: $Asx_{1.0}Phe_{1.0}Leu_{1.1}Pro_{1.0}Arg_{1.1}Ser_{0.9}Thr_{2.0}$. The cyclic analog cyclo(-Asn-Thr-Ser-Phe-Thr-Pro-Arg-Leu-) (cyclo[Asn^1]-LPK) was synthesized by Donzel's procedure (9) in 45% yield (nonoptimized) and purified by HPLC (retention time of 24.1 min), giving the same amino acid analysis: $Asx_{1.0}Phe_{1.0}Leu_{1.0}Pro_{1.1}Arg_{1.0}Ser_{0.9}Thr_{2.1}$. Fast-atom bombardment mass spectra were obtained on a VG-70/70 HS mass spectrometer (VG Organic, Manchester, U.K.) as described (10). Mass spectra showed that the parent MH^+ ion for the cyclic analog was 18 mass units less than the linear precursor: calculated for cyclo[Asn^1]LPK: 917.5 (MH^+); found: 917.4. Furthermore, while a strong ninhydrin response was observed showing a free amino in the linear precursor ([Asn^1]LPK-OH), cyclo[Asn^1]LPK demonstrated no such response.

The fragment Thr-Ser-Phe-Thr-Pro-Arg-NH_2 was synthesized by solid-phase methodology and found to be inactive on the cockroach hindgut bioassay (4), demonstrating the requirement for the C-terminal leucine residue for myotropic activity.

Structural Characterization of Cyclo[Asn^1]LPK by CD and NMR. CD spectra were taken on an Aviv model 61DS instrument (Aviv Associates, Lakewood, NJ) with a 1.0-mm sample cell (11) and were recorded at 50 μM concentration, pH 4.5, and 4.7°C.

The NMR spectra were acquired as described (12). Spectra acquired by double-quantum-filtered two-dimensional-correlated nuclear Overhauser effect (NOE) spectroscopy (NOESY) (13) and two-dimensional rotating-frame NOESY (ROESY) (14) on a Bruker MSL300 spectrometer were used to obtain complete assignments of all proton resonances in the peptide. The ROESY spectra (t_{mix} = 100–150 ms) were processed with linear baseline correction and t_1 ridge suppression. Amide proton temperature coefficients were calculated from the chemical shifts of the proton resonances, obtained from one-dimensional spectra at a series of temperatures, with the method of linear least squares. $^3J_{HN\alpha}$ (coupling constants between amide and C^α protons) were obtained from one- and two-dimensional spectra by direct measurement of peak-to-peak separation (15). Dioxan was used as an internal reference, but all chemical shifts are

Abbreviations: LPK, leucopyrokinin; NOE, nuclear Overhauser effect; NOESY, NOE spectroscopy; ROESY, rotating-frame NOESY; PBAN, pheromone biosynthesis-activating neuropeptide; cyclo[Asn^1]LPK, cyclo(-Asn-Thr-Ser-Phe-Thr-Pro-Arg-Leu-).

‡To whom reprint requests should be addressed.

Table 1. Distance constraints derived from NOE cross-peaks in the ROESY spectrum of cyclo[Asn[1]]LPK

Proton pairs	NOE interaction*
Asn-1C$^{\alpha}$H–Thr-2 NH	m†
Thr-2C$^{\alpha}$H–Ser-3 NH	m†
Ser-3C$^{\alpha}$H–Phe-4 NH	m†
Arg-7C$^{\alpha}$H–Leu-8 NH	m†
Asn-1 NH–Thr-2 NH	m†
Ser-3 NH–Phe-4 NH	m†
Arg-7 NH–Leu-8 NH	m†
Leu-8 NH–Asn-1 NH	s†
Thr-2C$^{\beta}$H–Ser-3 NH	s†
Ser-3C$^{\beta}$H–Phe-4 NH	m
Phe-4C$^{\beta}$H–Thr-5 NH	m
Thr-5C$^{\beta}$H–Pro-6 C$^{\delta}$H	m
Thr-5C$^{\alpha}$H–Pro-6 C$^{\delta}$H	m
Thr-2C$^{\alpha}$H–Phe-4 NH	vw†
Arg-7C$^{\alpha}$H–Asn-1 NH	vw†
Asn-1C$^{\alpha}$H–Phe-4 NH	w†
Thr-5C$^{\beta}$H–Leu-8 NH	vw
Thr-5C$^{\beta}$H–Arg-7 NH	vw
Thr-5C$^{\beta}$H–Leu-8C$^{\delta}$H	vw
Pro-6C$^{\beta}$H–Arg-7C$^{\beta}$H	vw

*Distances (d) are defined by: s = strong NOE, sum of van der Waals radii $< d <$ 2.5 Å; m = medium NOE, sum of van der Waals radii $< d <$ 3.5 Å; w = weak NOE, sum of van der Waals radii $< d <$ 4.5 Å; and vw = very weak NOE, sum of van der Waals radii $< d <$ 5.0 Å.

†Distance constraints used in the NOE-constrained molecular dynamics simulations of cyclo[Asn[1]]LPK. Medium and weak interactions involving side-chain atoms were not used.

quoted with reference to trimethylsilylpropanesulfonic acid at 0 ppm. Samples for NMR were ≈5 mM in peptide, were dissolved in 90% ^1H_2O/10% ^2H_2O, and were adjusted to pH 4.5 at 20°C with 5-μl volumes of 1 M NaOH and HCl.

Molecular Dynamics. Extended conformations of the peptides were built, energy-minimized, and subjected to molecular dynamics on Convex and Cray XMP supercomputers with the empirical potential-energy program DISCOVER and the graphics program INSIGHT (products of Biosym Technologies, San Diego) with force-field parameters as in ref. 16. Molecular dynamics were computed in time increments of 0.001 ps with a Verlet "leap-frog" algorithm (17). All potential energy calculations were done with both a full charge of +1 on the arginine side chain and with a neutralized arginine side chain. Because these simulations are done *in vacuo*, the electrostatic term due to the fully charged side chain is overemphasized. This effect was especially apparent in energy minimizations where the charged side chain often folded to interact with a peptide bond, forcing it out of planarity. The structures reported here were calculated with a neutral arginine side chain, but both types of simulation gave similar backbone conformations.

High-temperature molecular dynamics (150 ps) was done at a temperature of 600 K with minimization of the current conformation every 2 ps, resulting in 75 minimized structures. Minimized structures with root-mean-square (rms) deviations of their α carbon atoms between 0 and 0.5 Å were grouped into a single conformational family, and their similarity was verified visually by computer graphics. Eight distinct conformational families were found. Molecular dynamics (10 ps) was applied to selected structures from each family with NOE constraints (Table 1) represented as biharmonic functions with no energy penalty for distances between the lower (1.8 Å) and upper (2.5 Å, strong; 3.5 Å, medium; 4.5 Å, weak; 5.0 Å, very weak) bounds. Final structures were obtained by energy minimization. Structures from the high-temperature dynamics in the low-energy conformational family retained their original conformation and satisfied the NOE constraints (rms deviation of α carbon atoms less than 0.1 Å between the starting minimized high-temperature dynamics structure and the final structures minimized both with and without NOE constraints). Other structures from the high-temperature dynamics either adjusted their conformation to that of the low-energy conformational family upon application of the NOE constraints or retained high-energy conformations (>5 kcal·mol^{-1} above the lowest energy conformation). To test if the aqueous conformation would apply to the more hydrophobic bound environment of the receptor, solvent was excluded from the molecular dynamics simulations. Coordinates for the peptide will be supplied on request.

RESULTS AND DISCUSSION

Sequence Requirements Suggest Conformational Preferences. The known sequence requirements for pyrokinin activity provided the basis for conformational studies. All pyrokinins share the amide-blocked C-terminal sequence Phe-Xaa-Pro-Arg-Leu-NH_2 (Xaa = Ser, Thr, or Val), the "active core", that is both essential and sufficient for significant myotropic activity, as found by measurements of threshold concentrations for LPK and its analogs (8). The pyrokinin active core sequence can be aligned with other insect neuropeptides (Fig. 1), including the pheromone biosynthesis-activating neuropeptide (PBAN) (18, 19). Since PBAN shows pyrokinin-like myotropic activity (4) and the PBAN C-terminal decapeptide elicits pheromone biosynthesis (19), the pyrokinin C-terminal sequence is implicated in pheromone biosynthesis as well as hindgut and oviduct contractile activity. Removal of the C-terminal amino acid in both PBAN (19) and LPK eliminates all activity, further underscoring the similarity of these peptides. The existence of three naturally occurring sequences of the pyrokinin active core (Xaa = Ser, Thr, or Val) provided information on the role of specific amino acids and possible shared conformational preferences, while the small size of the active core allowed computational searches of conformational space.

Heliothis PBAN	Leu - Ser - Asp - Asp - Met - Pro - Ala - Thr - Pro - Ala - Asp - Glu - Glu - Met - Tyr - Arg - Glu - Asp - Pro - Glu - Glu - Ile - Asp - Ser - Arg - Thr - Lys - Tyr - **Phe - Ser - Pro - Arg - Leu - NH_2**
Locustamyotropin-I	Gly - Ala - Val - Pro - Ala - Ala - Gln - **Phe - Ser - Pro - Arg - Leu - NH_2**
Leucopyrokinin	pGlu - Thr - Ser - **Phe - Thr - Pro - Arg - Leu - NH_2**
Locustamyotropin-II	Glu - Gly - Asp - **Phe - Thr - Pro - Arg - Leu - NH_2**
Locustapyrokinin	pGlu - Asp - Ser - Gly - Asp - Gly - Trp - Pro - Gln - Gln - Pro - **Phe - Val - Pro - Arg - Leu - NH_2**

FIG. 1. Amino acid sequences of members of the pyrokinin family (leucopyrokinin from *Le. maderae* and locustamyotropin I, locustamyotropin II, and locustapyrokinin from the locust *Locusta migratoria*) and the pyrokinin-like PBAN aligned to show the common C-terminal pentapeptide sequence Phe-Xaa-Pro-Arg-Leu-NH_2 (Xaa = Ser, Thr, Val). PBAN from the silkworm is not pictured, but is of the same length and shares 27 of the 33 residues of the corn earworm (*Heliothis zea*) PBAN.

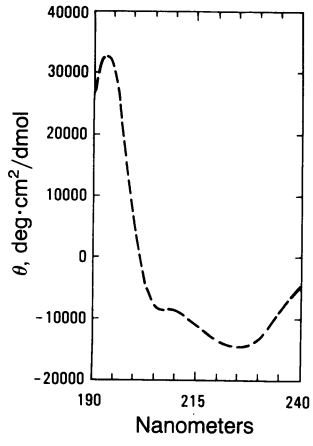

FIG. 2. CD spectrum of the conformationally constrained pyrokinin analog cyclo[Asn[1]]LPK, which exhibits a class C spectrum in water, consistent with the presence of a type I β-turn.

To design a constrained analog, we first examined the conformational preferences of the linear active core peptides. A turn structure within the active core was suggested by the presence of a proline residue and by secondary structure predictions (20) for the sequences Xaa-Pro-Arg-Leu (Xaa = Ser, Thr, or Val). During 200-ps molecular dynamics simulations, starting from the energy-minimized extended structures of *N*-Ac-Phe-Xaa-Pro-Arg-Leu-NH_2 (Xaa = Ser, Thr, or Val), the residues Xaa-Pro-Arg-Leu-NH_2 oscillated between an extended conformation and an open type I turn lacking a hydrogen bond between the first and fourth residues. Such flexibility is expected for small linear peptides, for which spectroscopic data cannot give explicit structural information, because the spectra represent a population-weighted average over all conformations (21).

Design, Synthesis, and Activity of a Conformationally Constrained Analog. To limit this flexibility, we designed and built a cyclic analog of LPK, cyclo[Asn[1]]LPK, starting from the observed open-turn conformation of the linear peptide *N*-Ac-Phe-Thr-Pro-Arg-Leu-NH_2 obtained from molecular dynamics. The *N*-acetyl group was replaced by the sequence Asn-Thr-Ser, and the torsion angles of these amino acids and the C-terminal leucine were adjusted with computer graphics to bring the C and N termini within 3 Å of each other, oriented to form a trans peptide bond. Neither attempts at bond closure during energy minimization or further computer graphics manipulation gave any additional structures with allowed torsion angles and trans peptide bonds. Energy minimization of this model resulted in a structure that differed significantly from the initial model (rms deviation between the α carbon atoms of the two structures = 2.1 Å) but maintained the type I β-turn between Thr-5 and Leu-8. During a further 100 ps of molecular dynamics followed by energy minimization, the β-turn structure of the backbone was maintained. The final energy-minimized structure had a saddle-shaped main-chain fold with approximate twofold symmetry with main-chain dihedral angles for Asn-1 and Thr-5 in the β region and for the other residues in the α region of (ϕ, ψ) space, and all trans peptide bonds. The backbone nitrogen and carbonyl oxygen atoms of Asn-1 and Thr-5 formed antiparallel β-strand hydrogen bonds across the middle of the saddle. The hydrogen bond between the Asn-1 backbone amide nitrogen and the Thr-5 backbone carbonyl oxygen closed a helical turn that included residues Thr-Ser-Phe at positions 2–4, while the hydrogen bond between the Thr-5 backbone amide nitrogen and the Asn-1 backbone carbonyl oxygen closed a second helical turn that included residues Pro-Arg-Leu at positions 6–8. An additional hydrogen bond from the Thr-5 carbonyl oxygen to the Leu-8 amide nitrogen closed the type I β-turn between these residues.

Since the computational studies indicated that the cyclic [Asn[1]]LPK analog would maintain a constrained β-turn conformation for the active core, cyclo[Asn[1]]LPK was synthesized. The N-terminal pyroglutamyl residue of LPK was replaced with asparagine because glutamine could self-condense into a pyroglutamyl moiety, blocking cyclization. Despite the rigidity imposed on its structure by cyclization, cyclo[Asn[1]]LPK, with a threshold response of 34 nM, retained a significant portion (about 1/24th) of the activity of its linear counterpart ([Asn[1]]LPK, 1.4 nM; ref. 8), which has a C-terminal amide as in LPK. The ease of cyclization under mild conditions indicated the intrinsic stability of cyclo-[Asn[1]]LPK. Cyclo[Asn[1]]LPK was 5 times more potent than its synthetic precursor, the linear C-terminal acid. Treatment of the linear acid and amide analogs with either immobilized aminopeptidase M (22) (cleaves peptides at the N terminus) or insoluble carboxypeptidase A (23) (cleaves peptides at the C terminus) destroyed all activity, while treatment of cyclo[Asn[1]]LPK did not affect activity or HPLC retention time. Thus, the activity of cyclo[Asn[1]]LPK was not due to trace amounts of precursor contaminants.

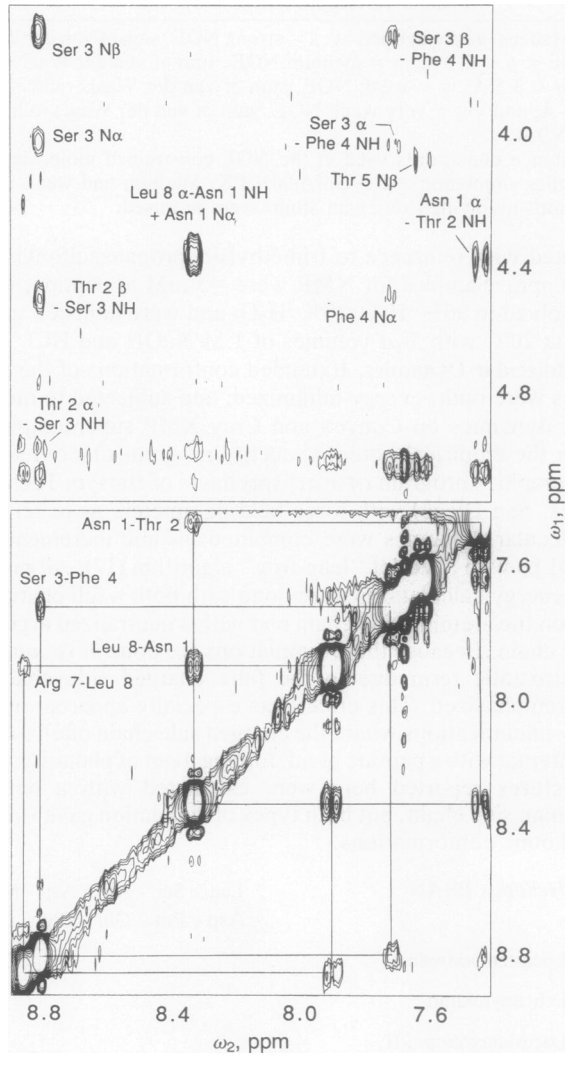

FIG. 3. Two portions of a 300-MHz ROESY spectrum (t_{mix} = 150 ms) of cyclo[Asn[1]]LPK. The amide diagonal region (*Lower*), showing the NOE cross-peaks between the amide protons, and the fingerprint region (*Upper*), showing the NOE cross-peaks between amide protons and the C^{α} protons, are plotted at the same contour level.

Active Conformation Confirmed by Physical and Computational Methods. The cyclo[Asn[1]]LPK conformation was characterized experimentally by CD to examine secondary structure and by proton NMR (ROESY) spectra to obtain NOE data on interproton through-space distances of <5 Å. The distinctive α-helix-like "class C" CD spectrum (Fig. 2) obtained from cyclo[Asn[1]]LPK in aqueous solution indicates either a type I or a type II′ β-turn in small cyclic peptides (13, 24, 25). NMR showed a strong NOE connectivity between the backbone amide protons of Asn-1 and Leu-8, confirming that the molecule was cyclic. NOE connectivities were observed between the C^{α} proton of Thr-5 and the C^{δ} protons of Pro-6 but not between the C^{α} protons of Thr-5 and Pro-6, indicating that the peptide bond between Thr-5 and Pro-6 was exclusively trans. The presence of a β-turn between Thr-5 and Leu-8 was shown by a sizable NOE connectivity between the amide protons of Arg-7 and Leu-8; the lack of a strong NOE connectivity between the C^{α} proton of Pro-6 and the amide proton of Arg-7 was consistent with a type I, rather than a type II, β-turn. Additional main-chain and side-chain distance constraints obtained from the ROESY spectrum (Fig. 3) are given in Table 1. Dihedral angles around the α carbon–nitrogen bonds of the polypeptide backbone were characterized by $^{3}J_{HN\alpha}$ coupling constants. The very large (for Thr-2, Thr-5, and Leu-8) and very small (for Ser-3 and Arg-7) coupling constants found indicated that the backbone of cyclo[Asn[1]]LPK was rigidly held in a single or a few closely related conformations, since conformational averaging would have given averaged, intermediate values. Temperature coefficients provided information on the solvent exposure of amide protons. The low-temperature coefficient (1.0×10^{-3} ppm/K) of the amide proton of Thr-2 indicated shielding from solvent, suggesting that this proton was involved in an intramolecular hydrogen bond. Those of Asn-1 (2.7×10^{-3} ppm/K), Thr-5 (3.4×10^{-3} ppm/K), Leu-8 (4.2×10^{-3}/K), and Phe-4 (5.4×10^{-3} ppm/K) showed increasingly greater solvent exposure. The large temperature coefficients of the Ser-3 (8.3×10^{-3} ppm/K) and Arg-7 (10.2×10^{-3} ppm/K) amide protons indicated complete exposure to solvent.

To incorporate the NMR data into our computationally based model, we searched the conformational space of cyclo[Asn[1]]LPK with high-temperature molecular dynamics starting from the energy-minimized molecular-dynamics-

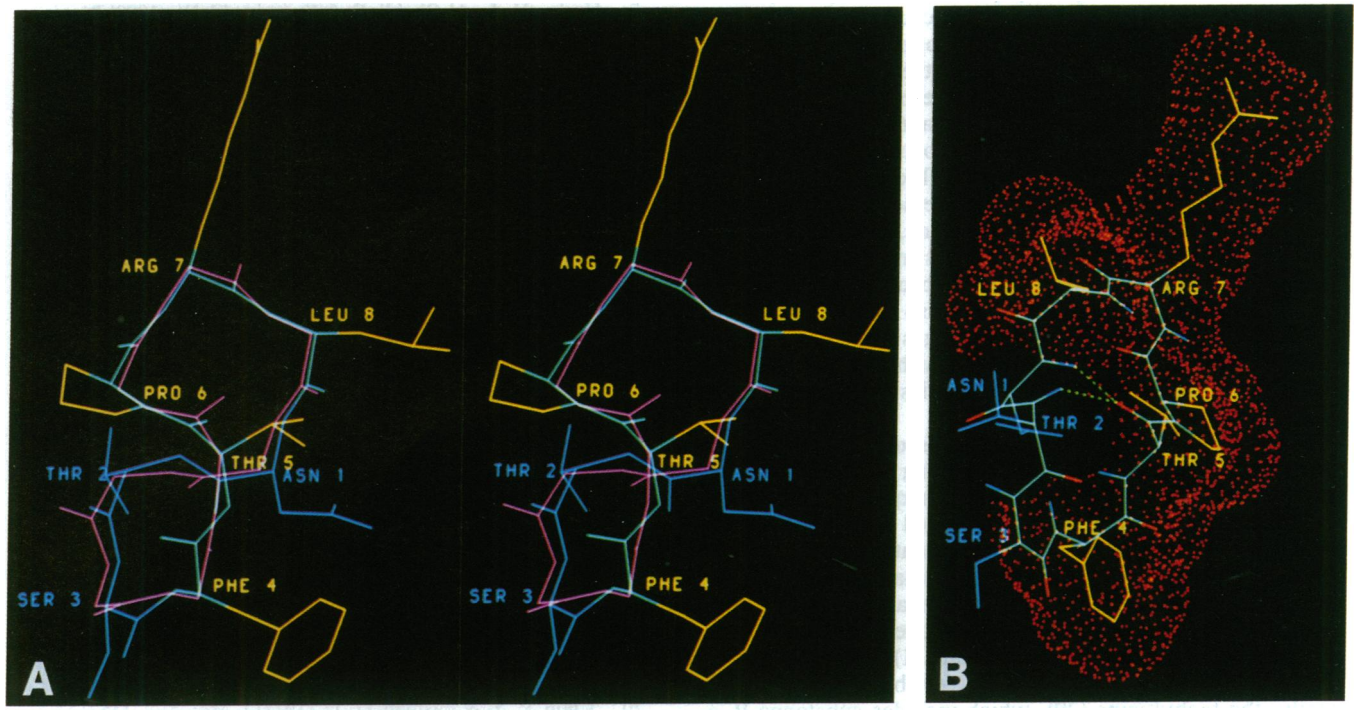

FIG. 4. Conformation of cyclo[Asn[1]]LPK. (*A*) A stereo pair of the superposition of the α carbon atoms of active-core residues Phe-4 to Leu-8 for two representative structures in the low-energy conformational family found for cyclo[Asn[1]]LPK. All structures in this low-energy family have a saddle-shaped main-chain fold and structurally similar active-core regions with a type I β-turn for residues Thr-5 to Leu-8. The amide protons of Ser-3 and Arg-7 extend away from the saddle-shaped backbone fold and into solvent, consistent with the large temperature coefficients seen for these protons. The backbone conformation shown in magenta is the energy-minimized molecular-dynamics-derived symmetrical structure. The other representative structure, with a light-blue main chain, yellow active-core side chains, and blue side chains for residues 1–3, shows that minor differences between the two structures occurred about non-active-core residue Thr-2. In particular, while residues Asn-1 to Phe-4 are in an approximate type I β-turn in the magenta structure ($\phi \approx -45°$, $\psi \approx -45°$ for Thr-2; $\phi \approx -75°$, $\psi \approx -45°$ for Ser-3) as part of the helical turn from Asn-1 to Thr-5, these residues are in an approximate type II′ β-turn ($\phi \approx 80°$, $\psi \approx -80°$ for Thr-2; $\phi \approx -80°$, $\psi \approx 15°$ for Ser-3) in the blue and yellow structure. Either a type I or a type II′ β-turn in this region would contribute to the class C CD spectrum in Fig. 2 (24–26) and is consistent with the backbone NOEs observed in this region (Table 1). Both structures satisfied all NOE main-chain constraints and predicted three hydrogen–hydrogen distances of <3 Å that were not seen as NOEs clearly in the ROESY spectrum in H_2O: two between the C^{α} proton of Thr-5 and the C^{δ} protons of Pro-6 (NOEs seen clearly in $^{2}H_2O$) and one between the amide protons of Phe-4 and Thr-5 (resonances have overlapping chemical shifts). (*B*) The molecular surface (27) of the active-core residues (red) is continuous because of the backbone conformation that causes the bonds between the α and β carbons of residues 4, 5, 7, and 8 to extend out from the polypeptide backbone in similar orientations. The surface was calculated for and is displayed with the yellow (active-core side chains) and blue structure in *A*. The main chain is light blue. Hydrogen bonds (green dashed lines) between main-chain amide protons (blue) and carbonyl oxygens (red) are also shown. The intramolecular hydrogen bond between the Thr-2 amide proton and the Thr-5 carbonyl oxygen diagonally connects the two lobes of the saddle, excluding the Thr-2 amide proton from solvent and providing an explanation for the very low temperature coefficient seen for this proton. A second hydrogen bond occurs between the Asn-1 amide proton and the Thr-5 carbonyl oxygen closing the helical turn containing Pro-Arg-Leu at positions 6–8.

derived conformation of the cyclic analog. Periodic minimization along the dynamics trajectory provided structures that were then categorized by conformation. All low-energy structures (within 5 kcal·mol^{-1} of the lowest energy structure found) fell in a single conformational family having the overall saddle-shaped fold and active core conformation of the starting structure. When structures from the conformational search (both high and low energy) were subjected to NOE-constrained (Table 1) molecular-dynamics simulations, all resulting low-energy conformations also belonged to this same family. Representative conformations of this family (Fig. 4*A*) showed the overall main-chain saddle-shaped fold with conservation of the structure in the active core region and minor structural variations about Thr-2, which is outside the active core. Thus, CD, NMR, and conformational searching by molecular dynamics were all consistent with one strongly preferred main-chain conformation (or a family of closely related conformations) for the active core. Although the precise conformation of the side chains of the active-core residues will be determined by the surrounding environment (aqueous versus receptor, for example), the active core main chain aligns these critical side chains to form one continuous surface on one side of the molecule (Fig. 4*B*).

The linear active-core pentapeptides can easily adopt the active-core β-turn conformation of the cyclic analog. Superposition of the α carbon atoms of the open β-turn structure obtained from molecular dynamics for the linear *N*-Ac-Phe-Xaa-Pro-Arg-Leu-NH_2 onto the corresponding atoms of cyclo[Asn^1]LPK demonstrated the similarity of the two structures (rms deviation of the α carbon atoms between the two structures of 0.23 Å). The much greater flexibility of the linear analogs probably accounts for their increased activity relative to the considerably more rigid cyclic analog, either because the active-core residues of the linear analogs are freer to adjust to the precise receptor configuration or because the residues outside the active core can move away so as not to interfere with binding. Although the cyclic analog is much less flexible than its linear counterpart, it is still highly active, and its well-defined backbone structure identifies the conformation necessary to interact with the receptor.

Implications for the Structural Basis of Neuroendocrine Functions. The eventual understanding of neuropeptide structure, chemistry, and function will require the combination of many approaches. The integrated approach used in this study will be useful for the elucidation of the active three-dimensional structures of other small peptides where the peptide sequence determines conformational preferences and hence the shape. Examples include the invertebrate neuropeptide families of the leucokinins (1), achetakinins (1), and locustatachykinins (28) and the vertebrate neuropeptide family, the tachykinins (29), which includes substance P, a possible link between the immune system and the nervous system. In the present study, we started from conformational analysis of the essential active-core pentapeptides, followed by combined experimental and computational approaches to design and define the stereochemistry of cyclo[Asn^1]LPK, a highly active, yet conformationally constrained analog of the pyrokinin insect neuropeptide family. The evidence from NMR and CD spectra and molecular dynamics identified a rigid β-turn conformation for the active core of cyclo-[Asn^1]LPK, suggesting that the active cores of the linear pyrokinins are in a similar β-turn conformation during interaction with the *Leucophaea* hindgut receptor. Since members of the pyrokinin and pyrokinin-like insect neuropeptide family also stimulate oviduct contraction and initiate pheromone biosynthesis, this biologically active β-turn conformation should be of significance to biological processes other than hindgut contraction. Determination of an active three-dimensional structure for the pyrokinin neuropeptide family provides a template for the design of peptide mimetics that actively inhibit or stimulate important peptide regulated functions, furthering the development of new, selective control measures against destructive insects.

We thank E. Getzoff and P. Wright for helpful discussion; W. S. Haddon for obtaining a mass spectrum; J. Cooper for technical assistance; J. Hicks and J. Lasch of PPG Industries (Pittsburgh); and R. Faust, J. Menn, D. Bull, and W. Newton of Agricultural Research Service, Department of Agriculture, for support of this work. This work was funded in part by National Science Foundation Grant 8822385 (to J.A.T. and V.A.R.) and PPG Industries.

1. Holman, G. M., Nachman, R. J. & Wright, M. S. (1990) *Annu. Rev. Entomol.* **35,** 201–217.
2. Kopec, S. (1917) *Bull. Int. Acad. Pol. Sci. Lett. Cl. Sci. Math. Nat. Ser. B,* 57–60.
3. Starratt, A. N. & Brown, B. E. (1975) *Life Sci.* **17,** 1253–1256.
4. Holman, G. M., Nachman, R. J., Schoofs, L., Hayes, T. K., Wright, M. S. & DeLoof, A. (1991) *Insect Biochem.,* in press.
5. Schoofs, L., Holman, G. M., Hayes, T. K., Tips, A., Nachman, R. J., Vandesaande, F. & DeLoof, A. (1990) *Peptides* **11,** 427–433.
6. Schoofs, L., Holman, G. M., Hayes, T. K., Nachman, R. J. & DeLoof, A. (1990) *Insect Biochem.* **20,** 479–484.
7. Hruby, V. J., Al-Obeidi, F. & Kazmierski, W. (1990) *Biochem. J.* **268,** 249–262.
8. Nachman, R. J., Holman, G. M. & Cook, B. J. (1986) *Biochem. Biophys. Res. Commun.* **137,** 936–942.
9. Donzel, B., Rivier, J. & Goodman, M. (1977) *Biopolymers* **16,** 2587–2590.
10. Nachman, R. J., Holman, G. M., Haddon, W. F. & Ling, N. (1986) *Science* **234,** 71–73.
11. Collawn, J. F., Wallace, C. J. A., Proudfoot, A. E. I. & Paterson, Y. (1988) *J. Biol. Chem.* **263,** 8625–8634.
12. Dyson, H. J., Rance, M., Houghten, R. H., Lerner, R. A. & Wright, P. E. (1988) *J. Mol. Biol.* **201,** 161–200.
13. Rance, M., Sørenson, O. W., Bodenhausen, G., Wagner, G., Ernst, R. R. & Wüthrich, K. (1983) *Biochem. Biophys. Res. Commun.* **117,** 479–485.
14. Bothner-By, A. A., Stephens, R. L., Lee, J., Warren, C. D. & Jeanloz, R. W. (1984) *J. Am. Chem. Soc.* **106,** 811–813.
15. Wüthrich, K. (1986) *NMR of Proteins and Nucleic Acids* (Wiley, New York).
16. Dauber-Osguthorpe, P., Roberts, V. A., Osguthorpe, D. J., Wolff, J., Genest, M. & Hagler, A. T. (1988) *Proteins* **4,** 31–47.
17. Hockney, R. W. & Eastwood, J. W. (1981) *Computer Simulations of Particles* (McGraw–Hill, New York).
18. Raina, A. K., Jaffe, H., Kempe, T. G., Keim, P., Blacher, R. W., Fales, H. M., Riley, C. T., Klun, J. A., Ridgeway, R. L. & Hayes, D. K. (1989) *Science* **244,** 796–798.
19. Kitamura, A., Nagasawa, H., Kataoka, H., Inoue, T., Matsumoto, S., Ando, T. & Suzuki, A. (1989) *Biochem. Biophys. Res. Commun.* **163,** 520–526.
20. Chou, P. Y. & Fasman, G. D. (1977) *J. Mol. Biol.* **115,** 135–176.
21. Dyson, H. J. & Wright, P. E. (1991) *Annu. Rev. Biophys. Biophys. Chem.* **20,** 519–538.
22. Royer, G. P. & Andrews, J. P. (1973) *J. Biol. Chem.* **248,** 1807–1812.
23. Cox, D. J., Bovard, F. C., Bargetzi, J.-P., Walsh, K. A. & Neurath, H. (1964) *Biochemistry* **3,** 44–47.
24. Deslauriers, R., Evans, D. J., Leach, S. J., Meinwald, Y. C., Minasian, E., Neméthy, G., Rae, T. D., Scheraga, H. A., Somorjai, R. L., Stimson, E. R., van Nispen, J. W. & Woody, R. W. (1981) *Macromolecules* **14,** 985–996.
25. Woody, R. W. (1985) *Peptides* **7,** 15–114.
26. Gierasch, L. M., Deber, C. M., Madison, V., Niu, C. H. & Blout, E. R. (1981) *Biochemistry* **20,** 4730–4738.
27. Connolly, M. L. (1983) *Science* **221,** 709–713.
28. Schoofs, L., Holman, G. M., Hayes, T. K., Kochansky, J. P., Nachman, R. J. & DeLoof, A. (1990) *Regul. Pept.* **31,** 199–212.
29. McGillis, J. P., Mitsuhashi, M. & Payan, D. G. (1990) *Ann. N.Y. Acad. Sci.* **594,** 85–94.